Characterization of Keto-Enol Tautomerism of Acetyl Derivatives from the Analysis of Energy, Chemical Potential, and Hardness

Patricia Pérez and Alejandro Toro-Labbé*

Departamento de Química Física, Facultad de Química, Pontificia Universidad Católica de Chile, Casilla 306, Correo 22, Santiago, Chile

Received: August 31, 1999; In Final Form: November 9, 1999

We present a theoretical study of the substituent effects on keto ⇌ enol equilibria in 10 acetyl derivatives (CH_3COX, X = H, OH, CH_3,OCH_3, NH_2, $N(CH_3)_2$, OCHO, F, Cl and Br). The analysis performed in terms of the potential energy, electronic chemical potential, and molecular hardness leads to the following results: (a) in the whole series, the keto isomers are more stable than the enol ones; (b) it is shown that the HSAB principle may explain the relative stability of the keto and the enol species; (c) accurate activation barriers are predicted from a modified Marcus-like equation that contains the force constants associated to reactants and products and to the imaginary frequency of the transition states; (d) the energy and hardness profiles are opposite to each other, verifying the principle of the maximum hardness.

1. Introduction

The tautomeric keto ⇌ enol and imine ⇌ enamine interconversions play a fundamental role in the mechanism of a number of organic synthesis processes,[1,2] biochemical processes, and enzymatic mechanisms.[2−6] This process is a rearrangement, in which a hydrogen migrates from the α-position with respect to a carbon−heteroatom double bond, to the heteroatom, thus forming a C−C double bond. In carbonyl-containing molecules, it has been established that in general, the keto tautomers are thermodynamically more stable than their enol counterparts by approximately 20 kcal/mol.[7−10] Chemical accuracy in the thermodynamics of keto ⇌ enol interconversion in these systems has recently become available, both in gas and solution phases. In the gas phase, there are still only limited experimental data available for the relative stabilities of the two forms.[11,12]

In the absence of a complete database of thermodynamics and kinetics aspects of the keto ⇌ enol equilibria, theoretical estimates of both relative stability and activation parameters are of special interest. There exist in the literature a number of ab initio studies that focus on these aspects of the keto ⇌ enol interconversion, that are directly comparable to gas-phase experimental results.[13−17] However, while the accuracy of thermodynamic data is determined by the ab initio method, reliable characterization of the transition state (TS) is crucial to assess the kinetic aspects. Recently, Lien et al.[18] reported an ab initio study of the keto ⇌ enol equilibria in α -substituted acetaldehydes to characterize the substituent effect at the α -carbon. These authors carried out a series of highly sophisticated ab initio calculations up to the G2 level to study the effect of a wide variety of substituents on the keto ⇌ enol equilibria. At different levels of theory, including electron correlation, they found that the keto-forms were systematically more stable than the enol forms. Energy barriers for the keto ⇌ enol conversion were found, ranging from 42.2 kcal/mol for the BH_2-substituted acetaldehyde to 65.2 kcal/mol for the F-substituted species, and a linear relationship between the activation energy and Hammett substituent resonance parameters was reported.[19]

An alternative way to probe substituent effects on these systems may be done in the frame of the global descriptors of reactivity, as electronic chemical potential μ and chemical hardness η, defined in the density functional theory (DFT) formulation of Parr, Pearson, and Yang.[20,21] Within this frame, thermodynamics as well as activation parameters may be successfully discussed within a representation that incorporates the simultaneous analysis of the energy, chemical potential, and hardness profiles.[22] It has been recently shown that the study of these global properties along a reaction coordinate is quite useful to rationalize the different aspects within the progress of chemical reactions.[22−26] In this context, the relationship between the hardness and energy profiles appears to be especially important to characterize transition states;[23−26] in particular, the principle of maximum hardness (PMH), which asserts that molecular systems at equilibrium tend to states of high hardness,[21,27−29] allows one to rationalize transition states through a minimum value of η, thus establishing a bridge connecting electronic and energetic properties, i.e., reaction mechanisms and thermodynamics. Since the initial proposal that the properties of the transition states should reflect in part those of reactants and products,[30,31] much work has been done about the rate-equilibrium concept and the application of linear free energy relationships. The Hammond postulate[32] is certainly the most important tool to get insights on the structure and properties of TSs from the knowledge of the structure and properties of reactants and products.

In this work, the keto ⇌ enol tautomerism of acetyl-derivatives CH_3COX (X = H, OH, CH_3, OCH_3, NH_2, $N(CH_3)_2$, OCHO, F, Cl and Br) will be characterized in terms of global and local properties. Global properties such as energy, μ and η will be used to describe different aspects of the keto ⇌ enol interconversion, including energy barriers and the effects of the substituent in the relative stability of the isomers. On the other hand, local quantities such as atomic charges and regional Fukui functions condensed to atoms will be used as descriptors of the charge-transfer associated to the proton migration. The properties of the corresponding TS structures will also be discussed.

* Corresponding author. E-mail: atola@puc.cl.

10.1021/jp9930797 CCC: $19.00
Published on Web 02/01/2000

2. Theoretical Background

General Definitions. We consider the keto ⇌ enol tautomerism as a chemical reaction of the type R → TS → P, where R represents the ground state of the keto form (reactant), P represents the ground state of the enol tautomer (product) and *TS* is the corresponding transition state. It is useful to connect R and P through a reduced reaction coordinate, ω, measuring the reaction progress in going from reactants ($\omega = 0$) to products ($\omega = 1$).[23−26,33] The reduced coordinate ω can be defined through a scaling procedure on the internal reaction coordinate (IRC) procedure obtained from ab initio calculations. An IRC calculation gives the reaction path leading down to reactants and products from the TS; at each step it optimizes the geometry of the system.

It is well-known that μ and η are the response of the system when the total number of electrons changes and the external potential $v(\vec{r})$ remains constant. Making use of a three-points finite difference approximation,[20,21] μ and η are defined as

$$\mu = \left[\frac{\partial E}{\partial N}\right]_v \approx -\left(\frac{I+A}{2}\right) \approx \frac{\epsilon_H + \epsilon_L}{2} \tag{1}$$

and

$$\eta = \frac{1}{2}\left[\frac{\partial \mu}{\partial N}\right]_v \approx \left(\frac{I-A}{2}\right) \approx \frac{\epsilon_L - \epsilon_H}{2} \tag{2}$$

where I is the first ionization potential and A the electron affinity. Koopman's theorem ($I = -\epsilon_H$, $A = -\epsilon_L$) allows one to write μ and η in terms of the energies of the frontier molecular orbitals HOMO (ϵ_H) and LUMO (ϵ_L) as indicated by the right-hand sides of eqs (1) and (2).

Transition State. In this work, the transition state will be characterized through its position along the reduced reaction coordinate at $\omega = \beta$ and by its own properties, the energy barrier $\Delta V^{\neq} = [V(\mathrm{TS}) - V(\mathrm{R})]$, the activation chemical potential $\Delta\mu^{\neq} = [\mu(\mathrm{TS}) - \mu(\mathrm{R})]$ and the activation hardness $\Delta\eta^{\neq} = [\eta(\mathrm{TS}) - \eta(\mathrm{R})]$. To rationalize the energy of the TS we use the Marcus equation:[23−26,33]

$$\Delta V^{\neq} \equiv V(\beta) = \left[\frac{1}{4}K_V + \frac{1}{2}\Delta V^o + \frac{(\Delta V^o)^2}{4K_V}\right] \tag{3}$$

where K_V is an intrinsic property of the reaction and $\Delta V^o = [V(1) - V(0)]$ is the energy difference between reactants and products.

The position of the transition state along the reduced reaction coordinate is related to the energy barrier through the Leffler's definition of the Brönsted coefficient (β):[34]

$$\beta \equiv \frac{\partial \Delta V^{\neq}}{\partial \Delta V^o} \Rightarrow \beta = \frac{1}{2} + \frac{\Delta V^o}{2K_V} \tag{4}$$

The TS is located at $\omega = \beta$, formally β measures the degree of resemblance of the TS to the product, and it is therefore quite useful to help rationalize the TS. It is important to note that β provides a quantitative basis to discuss the Hammond postulate:[32,34] if $\Delta V^o > 0$ then $\beta > 1/2$, and the transition state is closer to the products, whereas if $\Delta V^o < 0$, then $\beta < 1/2$, and the transition state is closer to the reactants.

3. Computational Methods

All calculations of the series of acetyl derivatives CH_3COX (X = H, OH, CH_3, OCH_3, NH_2, $N(CH_3)_2$, OCHO, F, Cl, and Br) were performed at HF/6-311G** level of theory using the Gaussian94 package.[35] The molecular structures along the IRC were fully optimized at the same level of theory. The profiles of V, μ and η were obtained through single points calculations of the fully optimized structures indicated by the IRC procedure. The chemical potential and hardness were computed using the HOMO and LUMO energies in eqs (1) and (2), respectively.

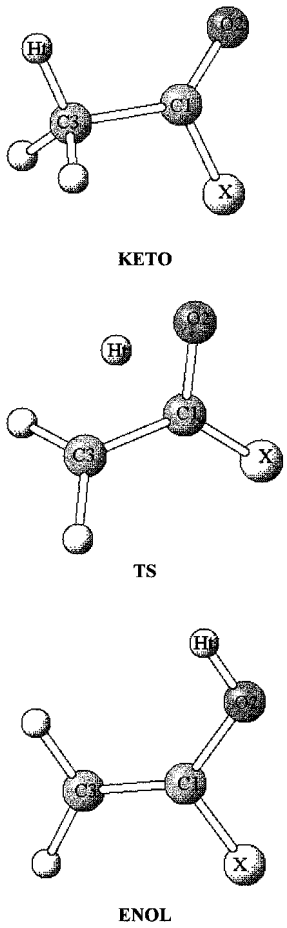

Figure 1. Representation of the keto, transition state, and enol structures involved in the keto ⇌ enol interconversion.

4. Results and Discussion

Global Properties. The stationary points of the energy surface for the keto ⇌ enol interconversion are sketched in Figure 1. Our first goal is to validate the methodology we use in this paper by comparing our calculated reaction potential energies [$\Delta V^o = V(\mathrm{enol}) - V(\mathrm{keto})$] with the DFT (B3LYP/6-31G**) values recently reported by Rappoport et al.[36] Both sets of energies are quoted in Table 1, where it can be seen that they are quite consistent; note that in all cases the keto forms are more stable than enol forms, in agreement with previous results,[7,8,13−19] Also, the order H < CH_3 < OCHO < Cl < Br < NH_2 ≈ $N(CH_3)_2$ < F < OH < OCH_3 in the relative stability is fairly well reproduced. Consistency between HF and DFT results is important because, in the absence of experimental data, some confidence in the numerical results is needed to assess the discussions of the following paragraphs on different aspects of the tautomeric rearrangement. In the following paragraphs, we will focus our attention on the energy changes in connection with the corresponding changes observed in electronic chemical potential and chemical hardness.

In Table 2, we display the reaction energy (ΔV^o), the energy barrier [$\Delta V^{\neq} = V(\mathrm{TS}) - V(\mathrm{keto})$], and the associated relative

TABLE 1: Comparison of the HF and DFT Relative Energies $\Delta V^o = [V(\text{enol}) - V(keto)]$ for the Series of Acetyl Derivatives CH_3COX[a]

X	ΔV^o HF/6-311G**	ΔV^{ob} B3LYP/6-31G**
H	12.6	13.1
OH	30.5	29.9
CH_3	14.3	14.9
OCH_3	32.5	29.6
NH_2	26.6	27.6
$N(CH_3)_2$	26.6	28.1
OCHO	23.8	23.2
F	28.0	27.0
Cl	24.4	25.0
Br	24.7	25.2

[a] All values are in kcal/mol. [b] Values reported in ref 36.

TABLE 2: Energy, Chemical Potential, and Hardness Values for the Keto ⇌ Enol Interconversion of Acetyl Derivatives CH_3COX[a]

X	ΔV^o	$\Delta\mu^o$	$\Delta\eta^o$	$\Delta V^{\neq}$	$\delta\Delta V^{\neq}$	$\Delta\mu^{\neq}$	$\Delta\eta^{\neq}$
H	12.6	22.9	−21.7	86.9	0.0	10.5	−38.8
OH	30.5	34.7	−40.6	89.9	3.0	30.3	−41.2
CH_3	14.3	23.2	−23.7	84.5	−2.4	18.7	−30.3
OCH_3	32.5	36.5	−37.8	89.0	2.1	34.1	−39.8
NH_2	26.6	33.6	−29.6	80.6	−6.3	26.6	−31.8
$N(CH_3)_2$	26.6	17.2	−13.7	76.7	−10.2	16.8	−19.6
OCHO	23.8	27.9	−26.9	91.6	4.7	23.7	−42.4
F	28.0	36.3	−42.8	94.8	7.9	33.0	−47.0
Cl	24.4	29.4	−28.5	94.0	7.1	18.2	−41.8
Br	24.7	20.0	−17.8	94.5	7.6	8.5	−28.7

[a] All values are in kcal/mol.

values in μ and η: $\Delta\mu^o = [\mu(\text{enol}) - \mu(\text{keto})]$, $\Delta\eta^o = [\eta(\text{enol}) - \eta(\text{keto})]$, $\Delta\mu^{\neq} = [\mu(\text{TS}) - \mu(\text{keto})]$ and $\Delta\eta^{\neq} = [\eta(\text{TS}) - \eta(\text{keto})]$. We first note that in all cases studied here $\Delta\eta^o < 0$, indicating that the most stable species (keto forms) are the hardest ones whatever the X substituent is; this is in agreement with the PMH.[21,22,27] Also, we note that $\Delta\mu^o > 0$; this entails that $\mu(\text{enol}) > \mu(\text{keto})$, indicating that the charge-transfer associated with the proton migration from keto to enol is, as expected, in the opposite direction to that of the proton motion.[37,38]

The substituent effects on the activation barriers may be analyzed with reference to the activation barrier for X = H. We define the activation barrier shift as $\delta\Delta V^{\neq} = \Delta V^{\neq}(\text{X}) - \Delta V^{\neq}(\text{H})$. This quantity is displayed in the sixth column of Table 2, and it will be used as a qualitative criterium to classify the different substituent as electron withdrawing or electron donating. It may be seen that methyl and amino groups present $\delta\Delta V^{\neq} < 0$, thus lowering the activation barrier with reference to X = H in the order: $N(CH_3)_2 > NH_2 > CH_3$. This is suggesting that the electron-donating character of these groups stabilizes the TS structure, lowering the energy barrier. In light of this result, one should expect that the electron-acceptor character of oxygen-containing and halogen groups push the energy barrier toward higher values with respect to X = H. The results of Table 2 show that this is correct and that the energy barrier increases in the order: F ≈ Br ≈ Cl > OCHO > OH > OCH_3. So qualitatively, a higher barrier seems to appear associated with the electron-withdrawing ability of the substituent that enhances the charge separation.

It is useful to qualitatively classify the interactions occurring among atoms in a molecule as being of the *through bond* or *through space* type. The first ones are expected to occur among partners that present similar local electronic populations, whereas the second ones are more related to nonbonded electrostatic interactions. Our results suggest that high barriers should be of the *through space* type, whereas low barriers are mainly of *through bond* type.[26,39]

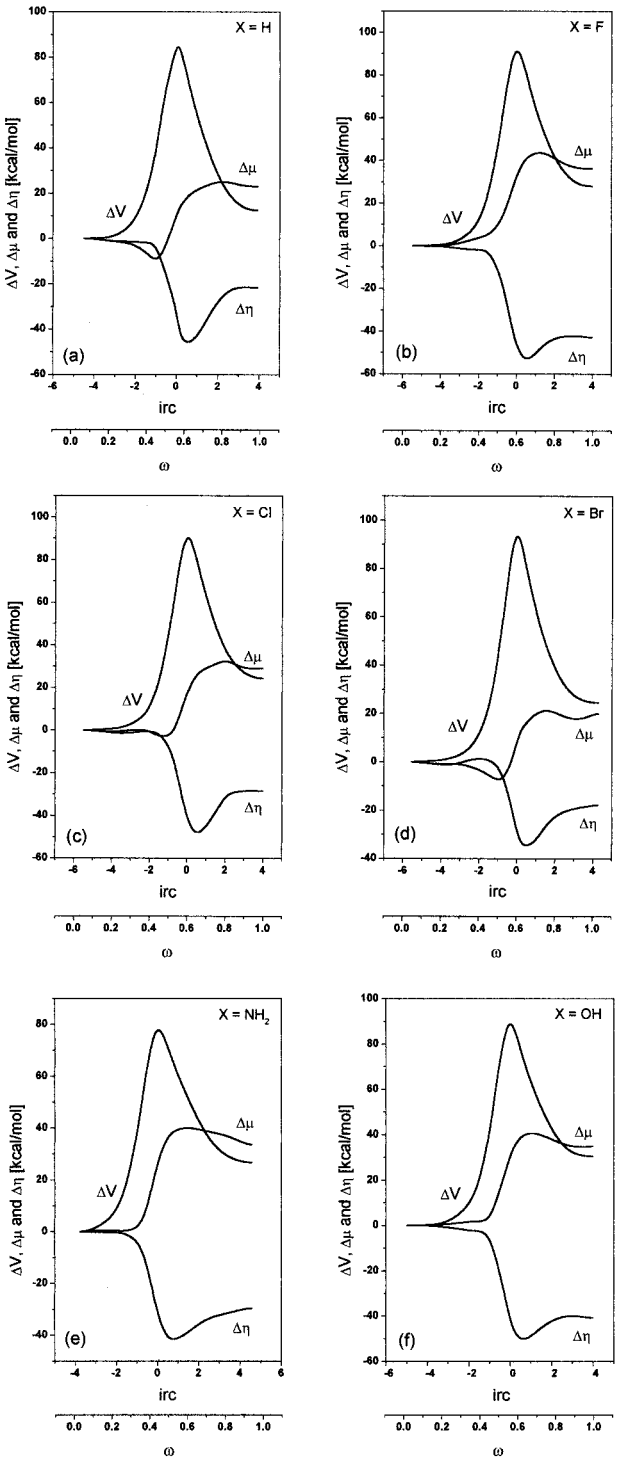

Figure 2. Potential energy, electronic chemical potential, and hardness profiles for the keto ⇌ enol interconversion of six representative acetyl derivatives: (a) X = H; (b) X = F; (c) X = Cl; (d) X = Br; (e) X = NH_2; and (f) X = OH.

On the other hand, Table 2 shows that for all substituent X, $\Delta\eta^{\neq}(\text{X}) < \Delta\eta^o(\text{X})$, indicating that at the TS, the hardness is a minimum; this is further evidence in favor of the PMH. Also $\Delta\mu^{\neq} > 0$ indicates that during the keto ⇌ enol interconversion there is a charge transfer from the TS to the keto ground state, in agreement again with what is expected to ocurr (electronic flux in the opposite direction to the proton migration).[37,38]

The Profiles of Energy, Chemical Potential, and Hardness. In Figure 2, we display the profiles of these properties along

TABLE 3: Transition State Parameters for the Keto ⇌ Enol Interconvertion of Acetyl Derivatives[a]

X	K_V	β	$k(\beta)$	k_{im}	λ	$\Delta V^{\neq}$	$\Delta V_o^{\neq}$	% error
H	321.9	0.5196	−160.7	584.2	−0.28	86.9	85.5	1.6
OH	295.5	0.5516	−146.2	525.3	−0.28	89.9	89.5	0.4
CH_3	308.7	0.5232	−154.0	550.7	−0.28	84.5	84.4	0.1
OCH_3	287.3	0.5566	−141.8	498.3	−0.28	89.0	90.1	1.2
NH_2	266.6	0.5499	−132.0	454.4	−0.29	80.6	83.0	2.9
$N(CH_3)_2$	250.8	0.5530	−124.0	427.4	−0.29	76.7	78.9	2.8
OCHO	317.0	0.5375	−157.6	564.5	−0.28	91.6	91.4	0.2
F	320.8	0.5436	−159.2	578.8	−0.28	94.8	93.4	1.5
Cl	325.4	0.5375	−161.8	606.6	−0.27	94.0	90.0	4.2
Br	326.7	0.5378	−162.4	609.1	−0.27	94.5	90.4	4.3

[a] All values are in kcal/mol.

the IRC for six selected representative acetyl derivatives, CH_3-COX with X = H, F, Cl, Br, NH_2 and OH. The keto forms are located at the negative values of the *IRC* (at $\omega = 0$). In all cases, the energy presents a quite sharp maximum representing the TS; μ and η also present a critical point at or very near the TS. The most relevant feature of Figure 2 is that η presents a nice opposite behavior with respect to the energy profile, confirming the validity of the PMH all along the reaction coordinate for the intramolecular proton transfer. Also, we observe that the variations of the chemical potential along the IRC (or ω) are intermediate between the variations of the potential energy and hardness; this is in agreement with previous results of chemical potential profiles for rotational isomerization and double-proton-transfer reactions.[25,26,39]

Characterization of the Transition State. As already mentioned, to get more insights into the transition state we have used the Marcus equation to rationalize the energy barrier for the proton transfer and have determined the K_V parameter using the optimized $\Delta V^{\neq}$ and ΔV^o values in eq 3; the results are quoted in Table 3. Note that $K_V > 0$ is an intrinsic property of the reaction, it has been shown that $K_V = (k_R + k_P)$ where k_R and k_P are the force constants associated to the potential wells of reactants and products.[26,33] The resulting K_V parameters have been used together with ΔV^o to obtain the Brönsted coefficient from eq 4. The third column of Table 3 shows the β values corresponding to the position of the TS along the reaction coordinate. We can see that in the whole series, the β values are greater than 1/2, and the TSs are closer to the products (enol form), in agreement with the Hammond postulate[32] for endoenergetic reactions. It is important to mention that the linear scaling procedure to determine the reduced reaction coordinate ω was performed for each individual IRC, and so they may differ from each other. In most cases, the scaling procedure located the energy maximum at ω values larger that 0.50, in agreement with the β values determined from eq 4. The only exception to this was X = NH_2; here, the maximum was found at $\omega < 0.50$. The flatness in the wings of the IRC profile of this system may be preventing an accurate scaling.

On the other hand, since the transition state corresponds to an energy maximum, the second derivative of the energy with respect to the reaction coordinate at the TS should be negative. Now, we assume that this second derivative evaluated at the transition state, $k(\beta)$, is related to ΔV^o and K_V through[26]

$$k(\beta) = \frac{1}{2}\left[\frac{(\Delta V^o)^2}{K_V} - K_V\right] \tag{5}$$

that comes out from the assumption that the TS results from interpolation of two armonic potentials associated to reactants and products and having individual force constants $k_R + k_P = K_V$.[26] The values of this new parameter characterizing the TS are given in Table 3, where we note that they are negative. We expect $k(\beta)$ to be related to the actual force constant (k_{im}) that is associated with the imaginary frequency defining the transition state structure that links the two minima. Values of k_{im}, determined from a standard frequency calculation, are also displayed in Table 3. Note that $k(\beta)$ and k_{im} are quantities that have been obtained independently; the first one comes from eq 5, whereas the second one is a product of a frequency calculation. The results for the 10 systems under study show that k_{im} and $k(\beta)$ are closely related through a constant $\lambda = k(\beta)/k_{im} \approx -0.28$; exact values of λ are also displayed in Table 3.

TABLE 4: Net Charges on Active Centers of the Keto ⇌ Enol Equilibria for Selected Acetyl Derivatives, in Electron Units

X	Q_{C3}(keto)	Q_{O2}(keto)
H	−0.2886	−0.3716
F	−0.2733	−0.3752
Cl	−0.2282	−0.3263
Br	−0.2324	−0.3119
NH_2	−0.2692	−0.4727
OH	−0.2510	−0.4466

The above result shows that it is possible to use k_{im} to obtain a new expression for the energy barrier, now containing a parameter accounting for a structural property of the optimized transition state. Combining eqs 3 and 5 and making use of the fact that $k(\beta) = \lambda k_{im}$, we define $\Delta V_0^{\neq}$ as

$$\Delta V_0^{\neq} = \frac{1}{2}[K_V + \lambda k_{im} + \Delta V^o] \tag{6}$$

Note that eq 6 is an expression for energy barriers that includes the force constants associated to the three relevant states along the reaction coordinate: reactants and products through $K_V = (k_R + k_P)$ and the TS through k_{im}. Values of $\Delta V_0^{\neq}$ are also quoted in Table 3, where it can be noticed that they are quite accurate when compared with the original $\Delta V^{\neq}$ values, with a maximum error of about 4%.

Population Analysis. It has been already established that the keto form is more stable than the enol form, whatever the substituent may be. This means that the favorable direction for the proton migration is from the enol to keto ground state. From a local point of view, it is then expected that the charge flux (Q) will take place from the keto to enol ground state, involving the C3 and O2 centers. A Mulliken population analysis reinforces the argument given previously concerning the charge transfer in terms of electronic chemical potential. In Table 4, the net charges on the active centers for the six selected representative cases are condensed.

In terms of the net charge, once the intramolecular proton transfer has taken place, the order $|Q_{C3}(\text{keto})| < |Q_{O2}(\text{keto})|$ is

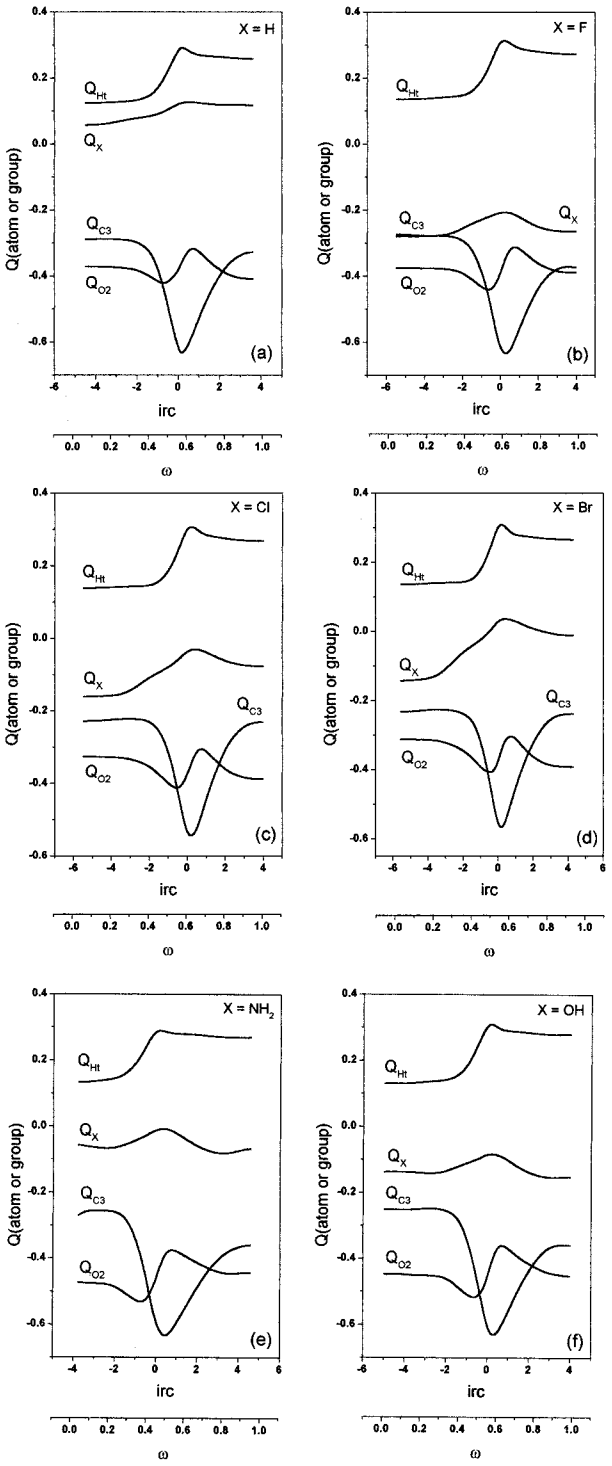

Figure 3. Net charges on relevant atoms or groups for the keto ⇌ enol interconversion of the selected acetyl derivatives: (a) X = H; (b) X = F; (c) X = Cl; (d) X = Br; (e) X = NH_2; and (f) X = OH.

expected, order that is conserved in consistency with the analysis performed from the difference in chemical potentials [μ(enol) > μ(keto)]. The analysis of the profiles of the electronic population of the relevant atomic centers involved in the reaction can be useful in understanding the specific interactions that determine the proton transfer. In Figure 3, we display the net charge profiles of the active C3 and O2 centers together with those of the substituent X and the transferred hydrogen Ht.

It is useful to perform the charge-transfer analysis for the keto ⇌ enol equilibria with reference to the TS structure. For X = H (Figure 3a), it may be seen that apparently there is no net charge transfer when we compare the keto and enol ground states for the C3 center. However, it may be observed that when going from the keto structure to the TS one, the C3 atom gains an important amount of electron density (ca 0.3372 electron units), and from the TS to the enol it loses an equivalent amount of the electron density (ca 0.2985 electron units), so that the net change between both ground states is marginal (ca −0.0387 electron units). The situation at the O2 center is opposite to that found at the C3 atom, although it is apparent that the charge-transfer effect at the O2 center takes place to a lesser extent. At the X = H atom, there are not significant variations, as expected. However, the transferred hydrogen Ht atom shows an increase in its positive charge, which attains a maximum value at the TS. It is also interesting to note that the Ht atom is more positively charged in the enol form than in the keto ground state, revealing a more polar character of the Ht−O2 bond as compared to Ht−C3 bond.

Figures 3b−3d display the charge transfer at the relevant centers for X = F, Cl and Br, respectively. While the picture at the C3, O2 and Ht centers remains quite the same as in Figure 3a, the charge variation pattern at the substituent shows an increasing charge transfer from the X atom in the order F < Cl < Br, as expected from the increasing softness pattern within the halogen series. Figures 3e and 3f show the charge transfer for the acetyl derivatives with X = NH_2 and X = OH, respectively. The picture displays for the active centers C3, O2 and Ht is approximately the same as the one displayed at the X = H. We observe a loss of charge on the groups X = NH_2 and X = OH in going from the keto ground state to the TS structure and then, from the vicinity of the TS to the enol species, these groups gain an amount of charge to attain an overall marginal gain of the enol form over the keto.

HSAB Analysis. A useful tool to analyze chemical reactivity is the well-known hard and soft acids and bases (HSAB) principle.[40] This empirical rule establishes that *hard−hard* or *soft−soft* interaction will proceed with a more favorable enthalpy change than the crossed interactions. This principle, which was formerly postulated on the basis of global softness and hardness, seems to be applicable at a local level,[41] where the appropiate descriptor to be used is the Fukui function $f(\vec{r})$, defined as the derivative of the electron density with respect to the number of electrons, at constant external potential.[20,21] This local reactivity index may be condensed to atoms or groups in a molecule. Its relevance in the context of the local HSAB rule comes from its exact relationship with local softness $s(\vec{r})$, namely $s(\vec{r}) = Sf(\vec{r})$, where S is the global softness, the inverse of the chemical hardness defined in eq 2. Since the global softness is a positive defined quantity, it follows that if $f_A < f_B$ then $s_A < s_B$ for any A, B pair of atoms or groups in a molecule.[42,43] In the present case, the pertinent atomic centers for the analysis of keto ⇌ enol equilibria are C3, O2, and Ht atoms. The Fukui function for these atomic centers was evaluated at the transition state structures using the local density approximation in which $f_A = \rho_A/N$, with ρ_A being the electronic population on atom A and N the total number of electrons. The results are displayed in Table 5.

It may be seen in all the cases considered that the Fukui function at the Ht center presents the lowest value when compared to those of the active C3 and O2 atoms; this in turn leads to the lowest local softness. Now, since the local softness is expected to be inversely proportional to the local hardness,[44] Ht becomes the hardest center among the three active atoms. Note that this is in agreement with the previous population analysis that showed the Ht atom having the maximum positive

TABLE 5: Condensed Fukui Functions at the Transition-State Structures for the Active Centers in the Series of Acetyl Derivatives CH_3COX

X	f_{Ht}	f_{C3}	f_{O2}
H	0.0297	0.2761	0.3494
OH	0.0216	0.2065	0.2642
CH_3	0.0223	0.1952	0.2630
OCH_3	0.0175	0.1650	0.2115
NH_2	0.0221	0.2063	0.2645
$N(CH_3)_2$	0.0148	0.1378	0.1767
OCHO	0.0150	0.1434	0.1829
F	0.0213	0.2021	0.2623
Cl	0.0173	0.1637	0.2095
Br	0.0120	0.1131	0.1444

charge at the TS. On the other hand, it may be seen in Table 5 that for all the cases considered, the Fukui function on the C3 site is systematically lower than that on the O2 site, indicating that at the TS, C3 is harder than O2. The hard-likes-hard part of the HSAB principle indicates that the reaction toward the keto form is favored, a situation that is confirmed thermodynamically: the keto form is more stable than the enol form. We conclude that the local HSAB principle applied to the TS structure may be used as a predictive tool to identify the favorable reaction channel.

5. Summary and Concluding Remarks

We have performed a theoretical study on the keto ⇌ enol tautomerism for a series of 10 acetyl derivatives CH_3COX. In all cases, we have found that the hardness profiles show a minimum value close to the position of the transition structures where the energy exhibits a maximum. This is evidence of the validity of the principle of maximum hardness in intramolecular proton-transfer reactions.

We have used the Marcus formula for rationalizing the energy barriers of the proton transfer processes; in doing so we have obtained an alternative new expression that depends parametrically on the force constants associated with reactants and products and with the imaginary frequency defining the transition-state structure. This expression predicts quite accurate energy barriers for the whole series and opens new ways to characterize the properties of transition states. The results validate the use of the Marcus equation for the analysis of this kind of chemical process.

The population analysis shows that once the intramolecular proton transfer has taken place, a charge flux between the active centers occurs in the opposite direction to the migration of the proton. We have used the local HSAB principle to show that the transferred proton (a hard species) may favorably interact with the hard carbon atom to give the most stable keto species.

Acknowledgment. This work was supported by FONDECYT through Projects No. 3990033 and 1990543 and by Cátedra Presidencial en Ciencias 1998 awarded to A.T.L.

References and Notes

(1) Hart, H. *Chem. Rev.* **1979**, *79*, 515.
(2) Rappoport, Z., *The Chemistry of Enols*; Wiley-Chichester, U.K., 1990.
(3) Alagona, G.; Desmeules, P.; Ghio, C.; Kollman, P. *J. Am. Chem. Soc.* **1984**, 106, 3623.
(4) Hupe, D. J. *New Comprehensive Biochemistry*; Page, M. I., Ed.; Elsevier: Amsterdam, 1984.
(5) Capon, B.; Guo, B. Z.; Kowk, F. C.; Siddhanta, A. K.; Zukko, C. *Acc. Chem. Res.* **1988**, *21*, 135.
(6) Johnson, W. P.; Gholamhossein, H.; Whitman, C. P. *J. Am. Chem. Soc.* **1992**, *114*, 11001.
(7) Lovering, L. *Can. J. Chem.* **1960**, *38*, 2367.
(8) Keefe, J. R.; Kresge, A. J.; Schepp, N. P. *J. Am. Chem. Soc.* **1988**, *110*, 1993.
(9) Saunders, W. H. *J. Am. Chem. Soc.* **1994**, *116*, 5400.
(10) Bernasconi, C. F.; Wenzel, P. J. *J. Am. Chem. Soc.* **1994**, *116*, 5405.
(11) Turecek, F.; Brabec, L.; Korvola, J. *J. Am. Chem. Soc.* **1988**, *110*, 7984.
(12) Keefe, J. R.; Kresge, A. J.; Schepp, N. P. *J. Am. Chem. Soc.* **1990**, *112*, 4862.
(13) Andrés, J.; Domingo, L. R.; Picher, M. T.; Safont, V. S. *Int. J. Quantum Chem.* **1998**, *66*, 9.
(14) Lee, D.; Kim, C. K.; Lee, B.-S.; Lee, I.; Lee, B. C. *J. Comput. Chem.* **1997**, *18*, 56.
(15) Bouma, W. J.; Radom, L.; Rodwell, W. R. *Theor. Chim. Acta* **1980**, *56*, 149.
(16) Zielinski, T. J.; Poirier, R. A.; Peterson, M. R.; Czismadia, I. G. *J. Comput. Chem.* **1982**, *1*, 62.
(17) Smith, B. J.; Nguyen, M. T.; Boums, W. J.; Radom, L. *J. Am. Chem. Soc.* **1991**, *113*, 6452.
(18) Su, C.-C.; Lin, C.-K.; Wu, C.-C.; Lien, M.-H. *J. Phys. Chem. A* **1999**, *103*, 3289.
(19) Wu, C.-C.; Lien, M.-H. *J. Phys. Chem.* **1996**, *100*, 594.
(20) Parr, R. G.; Yang, W. *Density Functional Theory of Atoms and Molecules*; Oxford University Press: New York, 1989.
(21) Pearson, R. G. *Chemical Hardness*; Wiley-VCH: New York, 1997.
(22) Chattaraj, P. K.; Nath, S.; Sannigrahi, A. B. *Chem. Phys. Lett.* **1993**, *212*, 223. Chattaraj, P. K.; Nath, S.; Sannigrahi, A. B. *J. Phys. Chem.* **1994**, *98*, 9143. Nath, S.; Sannigrahi, A. B.; Chattaraj, P. K. *J. Mol. Struct. (THEOCHEM)* **1994**, *309*, 65.
(23) Cárdenas-Jirón, G. I.; Lahsen, J.; Toro-Labbé, A. *J. Phys. Chem.*, **1995**, *99*, 5325.
(24) Cárdenas-Jirón, G. I.; Toro-Labbé, A. *J. Phys. Chem.* **1995**, *99*, 12730.
(25) Cárdenas-Jirón, G. I.; Gutiérrez-Oliva, S.; Melin, J.; Toro-Labbé, A. *J. Phys. Chem. A* **1997**, *101*, 4621.
(26) Gutiérrez-Oliva, S.; Letelier, J. R.; Toro-Labbé, A. *Mol. Phys.* **1999**, *96*, 61.
(27) Pearson, R. G. *J. Chem. Educ.* **1987**, *64*, 561.
(28) Datta, D. *J. Phys. Chem.* **1992**, *96*, 2409.
(29) Chattaraj, P. K. *Proc. Indian Natl. Sci. Acad.* **1996**, *62*, 513 and references therein.
(30) Evans, M. G.; Polanyi, M. *Trans. Faraday Soc.* **1938**, *34*, 11.
(31) Bell, R. P. *The Proton in Chemistry*; Cornell University Press: Ithaca, NY, 1973.
(32) Hammond, G. S. *J. Am. Chem. Soc.* **1955**, *77*, 334.
(33) Toro-Labbé, A. *J. Phys. Chem. A* **1999**, *103*, 4398.
(34) Leffler, J. E. *Science* **1953**, *117*, 340.
(35) Frisch, M. J.; Trucks, G. W.; Schlegel, H. B.; Gill, P. M. W.; Johnson, B. G.; Robb, M. A.; Cheeseman, J. R.; Keith, T. A.; Peterson, G. A.; Montgomery, J. A.; Raghavachari, K.; Al-Laham, M. A.; Zakrzewski, V. G.; Ortiz, J. V.; Foresman, J. B.; Ciolowski, J.; Stefanov, B. B.; Nanayakkara, A.; Challacombe, M.; Peng, C. Y.; Ayala, P. Y.; Chen, W.; Wong, M. W.; Andres, J. L.; Reploge, E. S.; Gomperts, R.; Martin, R. L.; Fox, D. J.; Binkley, J. S.; Defrees, D. J.; Baker, J.; Stewart, J. P.; Head-Gordon, M.; González, C.; Pople, J. A. Gaussian Inc.: Pittsburgh, PA, 1995.
(36) Sklenák, S.; Apeloig, Y.; Rappoport, Z. *J. Am. Chem. Soc.* **1998**, *120*, 10359.
(37) Scheiner, S. In *Hydrogen Bonding*; Truhlar, D., Ed; Oxford University Press: New York, Oxford, 1997.
(38) Pérez, P.; Contreras, R.; Vela, A.; Tapia, O. *Chem. Phys. Lett.* **1997**, *269*, 419.
(39) Jaque, P.; Toro-Labbé, A. *J. Phys. Chem. A* **2000**, in press.
(40) Pearson, R. G. In *Structure and Bonding 80: Chemical Hardness*; Sen, K. D., Ed.; Springer-Verlag: Berlin, Heidelberg, 1993 and references therein.
(41) Li, Y.; Evans, N. S. *J. Am. Chem. Soc.* **1995**, *117*, 7756.
(42) Pérez, P.; Contreras, R. *Chem. Phys. Lett.* **1998**, *293*, 239.
(43) Contreras, R.; Fuentealba, P.; Galván, M.; Pérez, P. *Chem. Phys. Lett.* **1999**, *304*, 405.
(44) Fuentealba, P. *J. Chem. Phys.* **1995**, *103*, 6571.